

RESEARCH ARTICLE

10.1002/2015MS000520

On the influence of poleward jet shift on shortwave cloud feedback in global climate models

Casey J. Wall¹ and Dennis L. Hartmann¹¹Department of Atmospheric Sciences, University of Washington, Seattle, Washington, USA

Key Points:

- High-latitude shortwave cloud feedback in GCMs driven by cloud microphysics, not jet shifts
- Inter-model differences in low cloud response to jet shift linked to shallow convection

Correspondence to:

C. Wall,
caseyw8@atmos.washington.edu

Citation:

Wall, C. J., and D. L. Hartmann (2015), On the influence of poleward jet shift on shortwave cloud feedback in global climate models, *J. Adv. Model. Earth Syst.*, 07, doi:10.1002/2015MS000520.

Received 20 JUL 2015

Accepted 23 NOV 2015

Accepted article online 26 NOV 2015

Abstract Experiments designed to separate the effect of atmospheric warming from the effect of shifts of the eddy-driven jet on shortwave (SW) cloud feedback are performed with three global climate models (GCMs). In each model a *warming* simulation produces a robust SW cloud feedback dipole, with a negative (positive) feedback in the high-latitudes (subtropics). The cloud brightening in high-latitudes that characterizes *warming* simulations is not produced by jet shifts alone in any of the models, but is highly sensitive to perturbations of freezing temperature seen by the cloud microphysics scheme, indicating that thermodynamic mechanisms involving the phase of cloud condensate dominate the SW feedback at high-latitudes. In one of the models a poleward jet shift causes significant cloud dimming throughout the midlatitudes, but in two models it does not. Differences in cloud response to jet shifts in two of the models are attributed to differences in the shallow convection parameterizations.

1. Introduction

The response of low clouds to climate change currently contributes the largest source of uncertainty to climate sensitivity in GCMs both globally [Boucher *et al.*, 2013] and in the midlatitude Southern Hemisphere (SH) [Ceppi and Hartmann, 2015], and has been the leading source of uncertainty for over 25 years [e.g., Cess *et al.*, 1990; Colman, 2003; Bony and Dufresne, 2005; Vial *et al.*, 2013]. In the SH extratropics, biases in radiatively important low clouds have been linked to the double Intertropical Convergence Zone bias [Hwang and Frierson, 2013] and to bias in the latitude of the eddy-driven jet [Ceppi *et al.*, 2012]. Historically, much attention has been given to studying cloud feedbacks in the tropics and subtropics [Boucher *et al.*, 2013, and references therein] and comparatively less attention has been given to low cloud feedbacks in the extratropics. It is therefore very important to study and improve the representation of SH extratropical low clouds and their feedbacks in models in order to reduce uncertainty in model predictions.

In addition to understanding cloud feedbacks, a long standing problem of great importance in climate science is improving our understanding of the interactions between clouds, radiation, and circulation, and how they change together in a warming climate [Bony *et al.*, 2015]. Other studies have claimed that in warming simulations in GCMs, to leading order, cloud changes drive midlatitude circulation changes and not the other way around [Ceppi *et al.*, 2014; Voigt and Shaw, 2015]. In this study we will address this problem by performing experiments designed to suppress feedbacks between clouds and circulation. By doing so we are able to examine causality between clouds and circulation changes in a changing climate.

Figure 1 shows the zonal-mean SW cloud feedback in a collection of 28 models from the Coupled Model Intercomparison Project Phase 5 (CMIP5). A robust feature of the meridional structure of SW cloud feedback in these models is a north-south dipole in the extratropics, with a positive feedback in the subtropics/lower midlatitudes ($\sim 20^{\circ}\text{S}$ – 40°S) and a negative feedback in the mid- to high-latitudes ($\sim 40^{\circ}\text{S}$ – 70°S). This dipole pattern is particularly robust in the Southern Hemisphere, where all 28 models agree on the negative sign of the SW cloud feedback over the Southern Ocean. Most models also predict a similar dipole response in the Northern Hemisphere. It is still an open question as to which mechanisms drive SW cloud feedback in the extratropics, and, in particular, the degree to which changes in large-scale atmospheric circulation are involved. We now list four mechanisms that have been proposed to explain the negative SW cloud feedback at mid- to high-latitudes.

© 2015. The Authors.

This is an open access article under the terms of the Creative Commons Attribution-NonCommercial-NoDerivs License, which permits use and distribution in any medium, provided the original work is properly cited, the use is non-commercial and no modifications or adaptations are made.

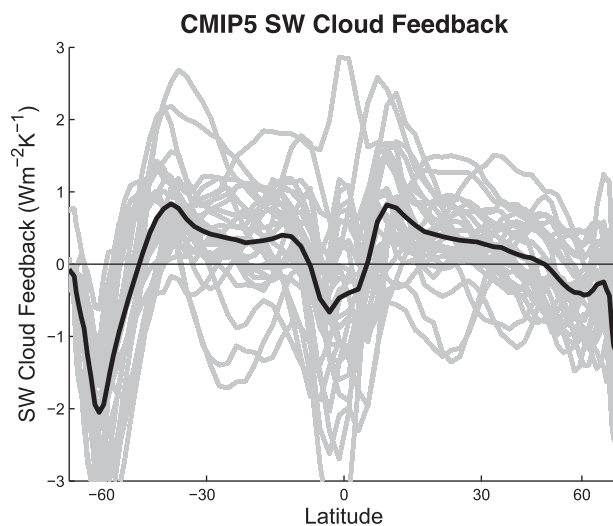


Figure 1. Zonal-mean SW cloud feedback from a collection of 28 CMIP5 models. The multimodel mean is shown in black and individual models are shown in grey. The abscissa is scaled by the sine of latitude. The feedback is computed using the method of Soden *et al.* [2008].

1.1. Poleward Shift of the Storm Tracks and Expansion of the Hadley Circulation

Poleward shift of the midlatitude eddy-driven jet has been proposed as a mechanism of the SW cloud feedback dipole pattern over the extratropics. CMIP5 models robustly predict a poleward shift of the midlatitude eddy-driven jet with warming [Barnes and Polvani, 2013]. Since the jet tends to follow regions of maximum baroclinicity, it has been claimed that the storm tracks and their associated clouds will migrate poleward with the jet, contributing to the negative SW cloud feedback at high-latitudes and positive feedback at lower latitudes [Tsushima *et al.*, 2006, Bender *et al.*, 2012, Grise *et al.*, 2013, Boucher *et al.*, 2013].

Recent studies have found that the importance of the jet shift mechanism on SH

cloud feedback varies between CMIP5 models. Kay *et al.* [2014] analyzed long integrations of the Community Earth System Model (CESM), which exhibits a SW cloud feedback dipole in warming simulations. In a preindustrial control simulation of CESM, they found only a weak absorbed shortwave response to natural variations in the jet latitude. They also found a small poleward jet shift in warming simulations compared to natural variability in the jet latitude in the preindustrial control run, and hypothesized that thermodynamic and near surface stability changes, not jet shifts, control SW cloud feedback over the Southern Ocean in CESM. Grise and Polvani [2014, hereinafter GP14] analyzed the response of SW cloud radiative effect (CRE) to natural variations in the jet latitude in 20 CMIP5 models. GP14 found that roughly half of the CMIP5 models show a zonally symmetric decrease in SW cloud reflection in the SH midlatitudes associated with a poleward jet shift, while in the other half of CMIP5 models, SW cloud reflection exhibits either a weak or zonally asymmetric pattern associated with a poleward jet shift. In abrupt CO₂ quadrupling experiments the average sea surface temperature over the Southern Ocean warms by ~1°C more after 100 years in the former class of models than in the later class of models, and the difference is statistically significant at the 90% confidence level (GP14). This result suggests that the jet shift mechanism may be significant in some models and not in others.

In observations, a significant trend in storm track clouds shifting poleward has been detected since the 1980s [Bender *et al.*, 2012], but it is uncertain how much of this trend was caused by increasing greenhouse gas concentrations, ozone depletion, changes in aerosol emissions, or other factors [Boucher *et al.*, 2013]. It is therefore difficult to assign an observational estimate to the SW cloud feedback due to a poleward jet shift. Other observational studies have found that SW cloud reflectivity over the Southern Ocean is weakly correlated or uncorrelated with the eddy-driven jet latitude [Ceppi and Hartmann, 2015; GP14]. This may be in part because over midlatitude oceans, high (low) cloud incidence is maximized in regions of large scale ascent (subsidence), so that changes in high and low cloud cover associated with jet shifts may partially cancel one another in the SW [Li *et al.*, 2014]. Longwave CRE, however, moves jointly with the eddy-driven jet, and both models and observations agree on this behavior [Ceppi and Hartmann, 2015; GP14].

It has also been proposed that changes in the Hadley circulation may drive low cloud feedback in the subtropics. CMIP5 models robustly predict that the Hadley circulation will weaken and expand poleward with global warming [Held and Soden, 2006; Tao *et al.*, 2015]. Weaker large-scale subsidence in the subtropics could cause the boundary layer top to rise [Bretherton *et al.*, 2013] or cause reduced entrainment of free tropospheric air of relatively low moist static energy into the boundary layer top [Brient and Bony, 2012], resulting in thicker or more abundant, and brighter low clouds. Some evidence suggests that change in large-scale subsidence alone is not a major contributor to subtropical low cloud feedback in GCMs, but it has not yet been ruled out [Bony *et al.*, 2004; Boucher *et al.*, 2013].

1.2. Changes in Condensate Phase in Mixed-Phase Clouds With Warming

The response of mixed-phase clouds to atmospheric warming has also been proposed as a thermodynamic mechanism to explain the negative SW cloud feedback in the mid- to high-latitudes. As the atmosphere warms, mixed-phase clouds favor the liquid over ice phase. As the ratio of ice crystal to liquid droplet number concentration decreases, the reflectivity of the cloud increases because liquid droplets tend to be smaller than ice crystals and because cloud lifetime increases. Ice crystals precipitate more efficiently than liquid droplets in mixed-phase clouds because ice crystals can rapidly grow at the expense of liquid droplets via the Bergeron process. Warming thus favors the formation of liquid droplets over ice crystals in mixed-phase clouds, and therefore reduces the overall precipitation efficiency of the cloud [Senior and Mitchell, 1993; Tsushima et al., 2006; Zelinka et al., 2012b]. Observational studies have also found this mechanism to be important over the midlatitude Southern Ocean, although models generally predict a negative SW cloud feedback over the Southern Ocean that is larger in magnitude than the observational estimate of the phase change feedback mechanism [McCoy et al., 2014]. However, the key physics of mixed-phase clouds are not well understood and likely not well represented in climate models, making this mechanism highly uncertain in models [Morrison et al., 2011; Boucher et al., 2013].

1.3. Increase in Adiabatic Cloud Water Content

Change in the slope of the moist adiabat with warming has been proposed as a mechanism of negative SW cloud feedback in the mid- to high-latitudes [Betts and Harshvardhan, 1987; Gordon and Klein, 2014]. The mass of cloud condensate formed in an updraft depends on the rate of change of the saturated water vapor mixing ratio with respect to height, which can be expressed as a function of the rate of change of potential temperature with respect to height following a moist adiabat (the “slope” of the moist adiabat). The slope of the moist adiabat is a strong function of temperature, and the rate of change of the slope of the moist adiabat with warming is roughly a factor of two larger in the mid- and high-latitudes than in the tropics. Because this mechanism is strongest at high-latitudes, previous studies have hypothesized that it may be an important mechanism for cloud brightening at mid- to high-latitudes with warming [Betts and Harshvardhan, 1987; Gordon and Klein, 2014]. However, this mechanism only accounts for changes in condensation in saturated updrafts, and many other processes can influence the radiative properties of clouds (e.g., changes in precipitation efficiency, phase of condensate, average depth of cloud, changes in circulation, etc.). Ceppi et al. [2015] found that in two GCMs, roughly two thirds of the change in liquid water path in the high-latitudes that resulted from warming is due to changes in the phase of condensate and weakening of microphysical processes that deplete cloud liquid. They concluded that, in models, negative SW cloud feedback at mid- to high-latitudes is driven primarily by changes in cloud microphysical processes, rather than changes in the slope of the moist adiabat. We will therefore not consider this mechanism in this study.

1.4. Changes in Frequency or Intensity of Midlatitude Storms

Tselioudis and Rossow [2006] used observations of SW CRE and sea level pressure, which they used as a metric for storm intensity, to quantify the radiative properties of clouds in midlatitude storms as a function of storm intensity. They then simulated a doubling of CO₂ with a climate model and used the changes in midlatitude storm frequency and intensity predicted by the model, along with their observational estimates of cloud radiative properties of storms, to estimate a cloud feedback associated with changes in frequency and intensity of midlatitude storms. The SW cloud feedback they estimated varied greatly between ocean basins and seasons. Other studies have claimed that this mechanism is not a driver of cloud feedback in the extratropics [Boucher et al., 2013]. This mechanism will not be addressed in this study.

In this study the “jet shift” and “phase change” mechanisms listed above are examined in three GCMs. The main questions addressed by this study are: (1) Are poleward jet shifts or phase changes in mixed-phase clouds important mechanisms for SW cloud feedback in the extratropics in GCMs? (2) Why does SW CRE have a relatively strong, zonally coherent response to natural variability in the jet latitude in some models and not in others, as noted by (GP14)? Simple experiments are performed with three GCMs in aquaplanet configuration to better understand the dipole pattern of SW cloud feedback in the Southern Hemisphere, and the extent to which poleward shifts of the eddy-driven jet are involved. The experiments demonstrate that the SW cloud feedback at high-latitudes is not driven by shifts in the eddy-driven jet, but responds strongly to perturbations in the freezing temperature seen by the cloud microphysics, indicating that the phase change mechanism dominates there. Shifts in the eddy-driven jet and the concomitant poleward

Table 1. Description of Models and Observational Data Used in this Study^a

Model/Observational Data Set Name	Description	Reference	SH Mean Jet Latitude ($\pm 2\sigma$) (°S)
<i>Aquaplanet Experiments:</i>			
<i>Jet Shift Experiments:</i>			
National Center for Atmospheric Research Community Atmosphere Model Version 5 (CAM5)	Aquaplanet configuration, "QOBS" SST profile	Neale et al. [2010a]	38.8 (± 3.9)
National Center for Atmospheric Research Community Atmosphere Model Version 4 (CAM4)	Aquaplanet configuration, "QOBS" SST profile	Neale et al. [2010b]	41.8 (± 3.0)
Geophysical Fluid Dynamics Laboratory Atmosphere Model Version 2.1 (AM2)	Aquaplanet configuration, "QOBS" SST profile	Anderson et al. [2004]	39.6 (± 3.3)
<i>Perturbed Microphysics Experiments:</i>			
CAM5	Aquaplanet configuration, "QOBS" + "FLAT" SST profiles	Neale et al. [2010a]	
AM2	Aquaplanet configuration, "QOBS" + "FLAT" SST profiles	Anderson et al. [2004]	
<i>CAM4-5 Progression Experiments:</i>			
CAM4	CAM4 physics, SSTs fixed to monthly climatology based on observations	See Gettelman et al. [2012] for control runs from "Modified Cess" experiments	51.6 (± 2.8)
CAM4-macro	Above + updated microphysics and macrophysics		51.1 (± 3.8)
CAM4-rad	Above + updated radiation		50.9 (± 3.8)
CAM4-aero	Above + updated aerosol		52.0 (± 2.8)
CAM4-shConv	Above + updated moist turbulence and shallow convection. Equivalent to CAM5 physics		50.7 (± 3.8)
<i>Observations/Reanalysis:</i>			
Clouds and Earth's Radiant Energy System (CERES)	Energy Balanced and Filled top-of-atmosphere fluxes version 2.7, SW CRE monthly mean from March 2000 to February 2014	Loeb et al. [2012]	
European Centre for Medium-Range Weather Forecasts Interim reanalysis (ERA-Interim)	Zonal wind monthly mean from March 2000 to February 2014	Dee et al. [2011]	50.6 (± 5.0)

^aThe SH jet latitude mean and standard deviation were computed over all months in the aquaplanet experiments (insolation was fixed to perpetual equinox values and SSTs did not vary in time in these experiments), and over DJF in CAM4-5 progression experiments and observations.

expansion of the Hadley circulation have a more uncertain influence on SW cloud feedback in the lower midlatitudes. In two of the models, jet shifts have little influence on cloud brightness, while in one model a poleward jet shift causes a significant dimming of clouds throughout the midlatitudes. The different cloud response to a poleward jet shift between two of the models in this study is shown to result from differences in shallow convection and moist turbulence parameterizations. This paper is organized as follows: experimental setup and data are described in section 2, results and discussion in section 3, and concluding remarks in section 4.

2. Experimental Setup

Three models were used in this study: the Geophysical Fluid Dynamics Laboratory Atmosphere Model Version 2.1 and the National Center for Atmospheric Research Community Atmosphere Model Version 5 and Version 4, henceforth referred to as AM2, CAM5 and CAM4 respectively. A progression of model configurations building up from CAM4 to CAM5 was also used to attribute the different cloud response to jet shifts in the two models to differences in shallow convection and moist turbulence parameterizations. Finally, observations of SW CRE from the Clouds and Earth's Radiant Energy System (CERES) experiment and zonal wind from the European Centre for Medium-Range Weather Forecasts Interim reanalysis (ERA-Interim) were used (see Table 1).

The goal of this modeling study is to separate the contribution made to SW cloud feedback by changes in large-scale atmospheric circulation from the contribution made by changes in mixed-phase cloud

microphysics. To accomplish this, two sets of experiments were performed: Jet Shift Experiments in which the jet is forced to shift poleward with little change in the atmospheric temperature, and Perturbed Microphysics Experiments in which the freezing temperature seen by the cloud parameterizations is perturbed. These experiments are designed to approximately isolate the jet shift and phase change mechanisms, respectively. All experiments were run in fixed-SST aquaplanet configuration, and were modeled after previous aquaplanet intercomparison studies [e.g., Neale and Hoskins, 2000; Taylor et al., 2012; Blackburn and Hoskins, 2013; Medeiros et al., 2014]. Because SST is prescribed in all experiments, the ability of cloud changes to feed back on the atmospheric circulation is greatly diminished. The experiments therefore allow us to estimate the extent to which circulation changes and thermodynamic changes cause changes in cloud brightness. However, we emphasize that this approach is not able to capture the interactions among cloud feedback, SST and circulation that are known to be important. In these experiments it is our goal to specify the circulation change and see to what extent it affects the cloud properties.

Aquaplanet models are useful for understanding processes that control cloud feedbacks. Previous studies have found that aquaplanet models and their more realistic counterparts respond similarly to warmer SSTs and quadrupled CO₂ forcing. Aquaplanet models and models in the Atmospheric Model Intercomparison Project (AMIP) configuration exhibit similar large-scale circulation responses to SST warming and quadrupled CO₂ forcing, including a wider, weaker Hadley circulation and a poleward migration of the eddy-driven jet [Medeiros et al., 2014]. Additionally, Medeiros et al. [2008] argued that AM2 and the National Center for Atmospheric Research Community Atmosphere Model Version 3, a precursor of CAM4 and CAM5, are “best case scenario” models in which the aquaplanet configuration is a useful testing ground for understanding cloud feedback in more realistic model configurations.

The “control” setup for the aquaplanet experiments is described below, and unless otherwise stated the parameters remain constant through all experiments. Insolation was set to perpetual equinox conditions with a diurnal cycle, sea ice was neglected, and greenhouse gas concentrations were set to preindustrial levels. Experiments were run for 6 years, and zonal and temporal averages of the last 4 years are analyzed. Two different SST profiles were used: “QOBS” and “FLAT” [see Neale and Hoskins, 2000] for a complete description of the profiles). Both profiles are zonally symmetric with a maximum of 27°C on the equator and 0°C poleward of 60° N/S. “QOBS” has the advantage of being commonly used in previous aquaplanet studies [e.g., Medeiros et al., 2014] and is the only aquaplanet experiment included in the CMIP5 archive [Taylor et al., 2012]. It has the disadvantage, however, of having a significant equatorward bias in the eddy-driven jet latitude. The “FLAT” profile has a much smaller bias in the jet latitude and higher baroclinicity in the extratropics compared to the “QOBS” profile. Our major conclusions are not sensitive to the choice of SST profile.

2.1. Jet Shift Experiments

In each model, *control*, *warming*, and *torque* experiments were performed. The setup for *control* is described in the previous paragraph. In *warming*, the SST profile was warmed uniformly by 4K, and in *torque* the model was forced with a prescribed zonally symmetric steady zonal wind tendency in the midlatitude upper troposphere with the SSTs locked to *control* values. The zonal wind tendency was tuned such that the response of the mean meridional overturning circulation and latitude of the eddy-driven jet in the *torque* experiment was as close as possible to that in the *warming* experiment (see Appendix A for a detailed description of the *torque* forcing). The *torque* experiment is able to approximately reproduce the poleward shift of the eddy-driven jet and response in zonal-mean, time-mean vertical velocity between 30° and 70°S of the *warming* experiment, but does so with a very small temperature change compared to the *warming* experiment (Figures 2 and 3). The jet shifts in the *warming* and *torque* experiments in all models are found to be statistically significant at the 95% confidence level (from a Student’s *t*-test) when compared to the *control* experiment. The “QOBS” SST profile was used in the experiments described below.

We will now discuss the similarity in the large scale circulation response between the *torque* and *warming* experiments. In order to quantify the similarity between the large-scale vertical velocity response in the extratropical lower troposphere (30°S–70°S and below 500 hPa) between the *warming* and *torque* experiments ($\Delta\omega^{gw}$, $\Delta\omega^{tor}$ respectively) for a given model we employ the mass-weighted correlation and normalized root mean square error (NRMSE) relative to the *warming* response:

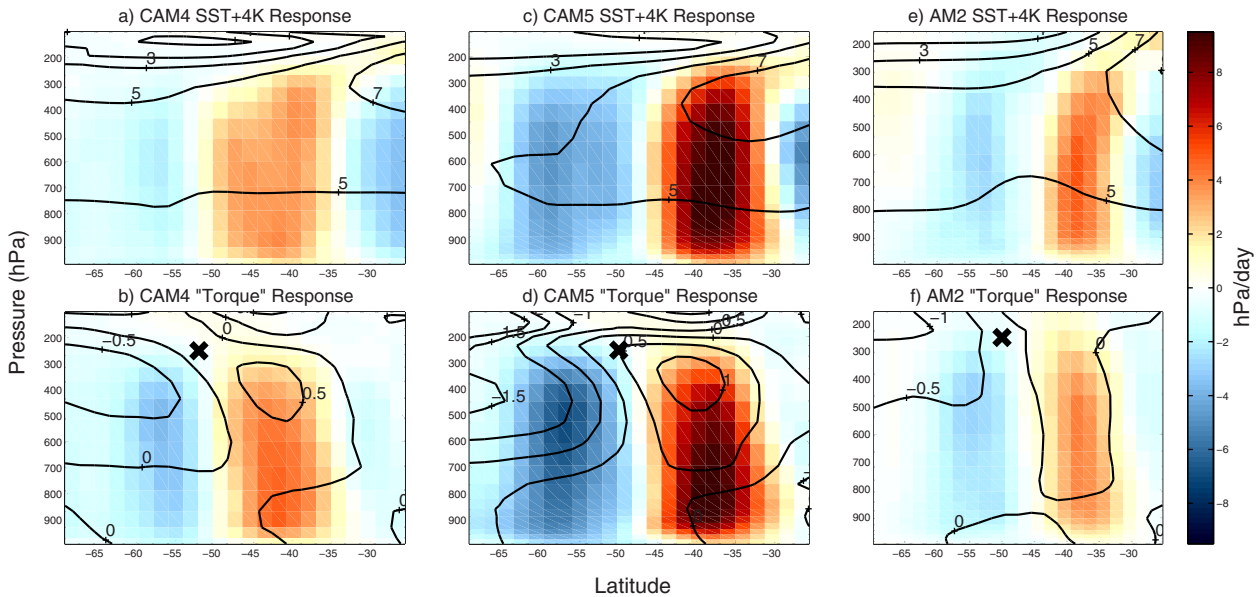


Figure 2. Zonal-mean time-mean vertical pressure velocity (color) and atmospheric temperature (contours, units: °C) response in the (a) *warming* and (b) *torque* experiments in CAM4. The “X” in Figure 2b shows the center of the zonal wind tendency applied in the *torque* experiment. (c–f) As in Figures 2a and 2b but for CAM5 and AM2, respectively. Note the similarity in ω response and the difference in atmospheric temperature response between the *warming* and *torque* experiments in all three models.

$$\text{NRMSE}(\Delta\omega^{gw}, \Delta\omega^{tor}) = \frac{\sqrt{N^{-1} \sum_{\phi=30^{\circ}S}^{70^{\circ}S} \sum_{p=1000}^{500} \text{hPa} (\Delta\omega_{\phi,p}^{gw} - \Delta\omega_{\phi,p}^{tor})^2}}{\max(\Delta\omega^{gw}) - \min(\Delta\omega^{gw})}$$

where the maximum and minimum terms are taken over the same region as the sum and N is the number of gridpoints. The correlation and NRMSE are measures of similarity in the spatial pattern and magnitude of the response in the *torque* and *warming* experiments, respectively. In the extratropical lower troposphere, the mass-weighted correlation coefficient (NRMSE) between $\Delta\omega^{gw}$ and $\Delta\omega^{tor}$ ranges between 0.92 and 0.99

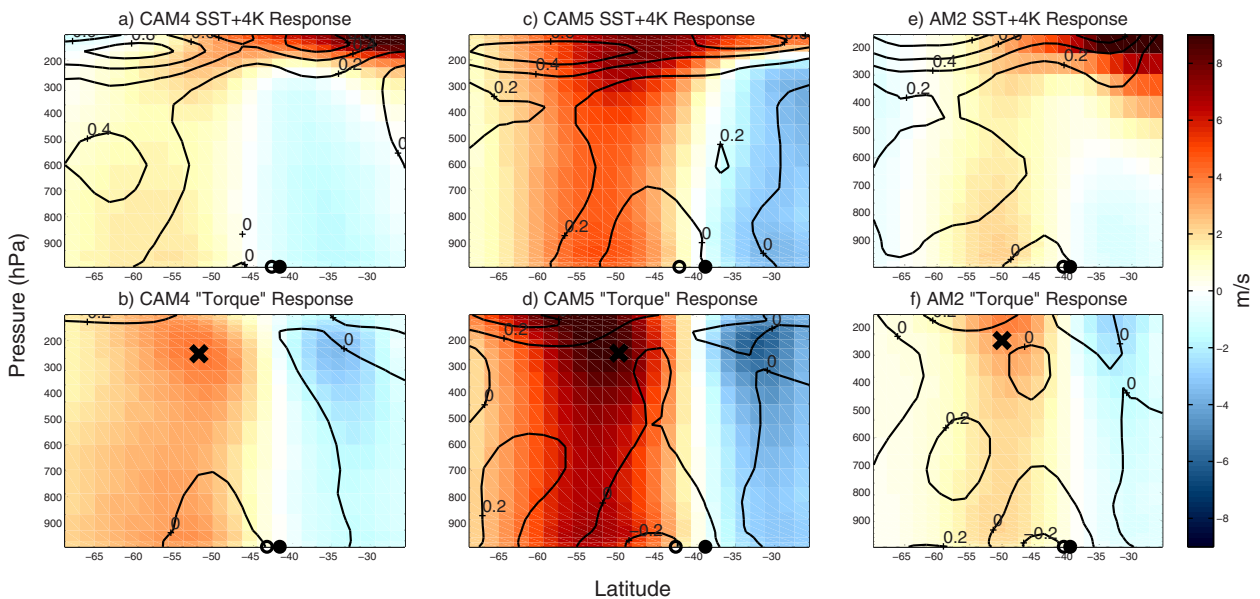


Figure 3. Zonal-mean zonal wind response in the (a) *warming* and (b) *torque* experiments in CAM4. Colors indicate the mean zonal wind response, contours show the fractional change in variance, and closed (open) circles on the abscissa show the jet latitude in the *control* (*warming*/*torque*) experiments. The “X” in Figure 3b shows the center of the zonal wind tendency applied in the *torque* experiment. (c–f) As in Figures 3a and 3b but for CAM5 and AM2, respectively.

Table 2. Comparison of the Circulation Response in the *Torque* and *Warming* Simulations in Jet Shift Experiments^a

	$\Delta\bar{w}$	$\Delta\bar{u}$	Poleward Jet Shift (°S)
CAM5	$r=0.99$ NRMSE =0.06	$r=0.99$ NRMSE =0.17	<i>warming</i> : 3.3 <i>torque</i> : 3.8
CAM4	$r=0.92$ NRMSE =0.14	$r=0.96$ NRMSE =0.32	<i>warming</i> : 1.0 <i>torque</i> : 1.6
AM2	$r=0.97$ NRMSE =0.08	$r=0.96$ NRMSE =0.13	<i>warming</i> : 1.1 <i>torque</i> : 1.0

^aBoth the mass weighted correlation coefficient (r) and normalized root mean square error (NRMSE, described in text) in the midlatitude lower troposphere (30°S–70°S, below 500 hPa) are shown for each model. $\Delta\bar{w}$ ($\Delta\bar{u}$) indicates the zonal-mean, time-mean response of the vertical (zonal) velocity. The poleward jet shift in both experiments is also shown.

torque experiment. Figure 3 shows changes in both the mean and variance of the zonal wind and the jet latitude in the *torque* and *warming* experiments. The jet latitude is computed by fitting a quadratic to the maximum zonal-mean zonal-wind at 850 hPa and the two neighboring latitude points, and then finding the latitude of maximum wind of the quadratic fit (see Appendix A). In the midlatitude lower troposphere (30°S–70°S, below 500 hPa) the mass weighted correlation (NRMSE) between the mean zonal wind response in *torque* and *warming* experiments ranges between 0.96 and 0.99 (0.13–0.32) (Table 2). The higher NRMSE values occur because the mean zonal wind response is generally larger in magnitude in the *torque* experiment than in the *warming* experiment. This is to be expected, because the zonal wind tendency applied in the *torque* experiment is a net source of zonal momentum to the atmosphere. In the upper troposphere, however, there is a clear increase in the mean and variance of the zonal wind in the *warming* experiment that is strongest at lower latitudes and occurs because the tropopause height rises, and this effect is not present in the *torque* experiment. We do not expect the raised troposphere in the tropics to effect the SW cloud feedback in midlatitudes very much, though. Also, the jet shift in the *torque* and *warming* experiments is similar in all three models (Table 2).

In summary, the large scale vertical velocity response and poleward jet shift are very similar in the *torque* and *warming* experiments. The zonal wind response in the middle and lower troposphere is highly correlated between the two experiments, but generally larger in magnitude in the *torque* experiment than in the *warming* experiment. The zonal wind response in the upper troposphere is quite different between the *torque* and *warming* experiments because the *torque* experiment is not able to recreate the deepening of the troposphere that occurs in the *warming* simulations. However, because the circulation response in the lower and middle troposphere in the midlatitudes is very similar between the *torque* and *warming* simulations, and because SW cloud forcing [Haynes et al., 2011; McCoy et al., 2014] and feedback [Kay et al., 2014] over the Southern Ocean are dominated by low clouds, the *torque* experiment allows us to estimate the extent to which circulation changes drive SW cloud feedback in the midlatitudes in the aquaplanet models.

2.2. Perturbed Microphysics Experiments

In the Perturbed Microphysics Experiments, the experimental setup was the same as in the *control* experiment of the Jet Shift Experiments except the freezing temperature seen by the cloud ice parameterizations was perturbed following the method of Ceppi et al. [2015]. Freezing temperature perturbations ranged between -4°C and $+4^{\circ}\text{C}$ in increments of 1°C , and experiments were run with and without a uniform SST warming of $+4\text{K}$ for each value of freezing temperature perturbation.

Freezing temperature perturbations were implemented in all portions of the code that compute sources and sinks of cloud ice, including parts of the cloud microphysics, cloud macrophysics and convection schemes. This was done by changing the freezing temperature seen by all relevant sections of the code and changing the saturation vapor pressure seen by the Bergeron process. The cloud ice processes generate (deplete) cloud ice only for temperatures below (above) certain threshold values, some of which are different from 0°C . For example, homogeneous freezing of cloud droplets occurs at temperatures below -40°C in CAM5. All temperature threshold values for cloud ice processes were perturbed by the same amount as the freezing temperature. Henceforth we will refer to the temperature perturbations applied to the cloud ice processes as “freezing temperature perturbations” for brevity.

(0.06–0.14) between models (Table 2). However, in the *warming* experiment the atmosphere warms by $\sim 5\text{K}$ throughout the troposphere, while in the *torque* experiment the atmospheric warming is at least an order of magnitude smaller (Figure 2).

The zonal wind response is similar between the *torque* and *warming* experiments in the middle and lower troposphere, but the *warming* experiment exhibits a deepening of the troposphere that is not present in the

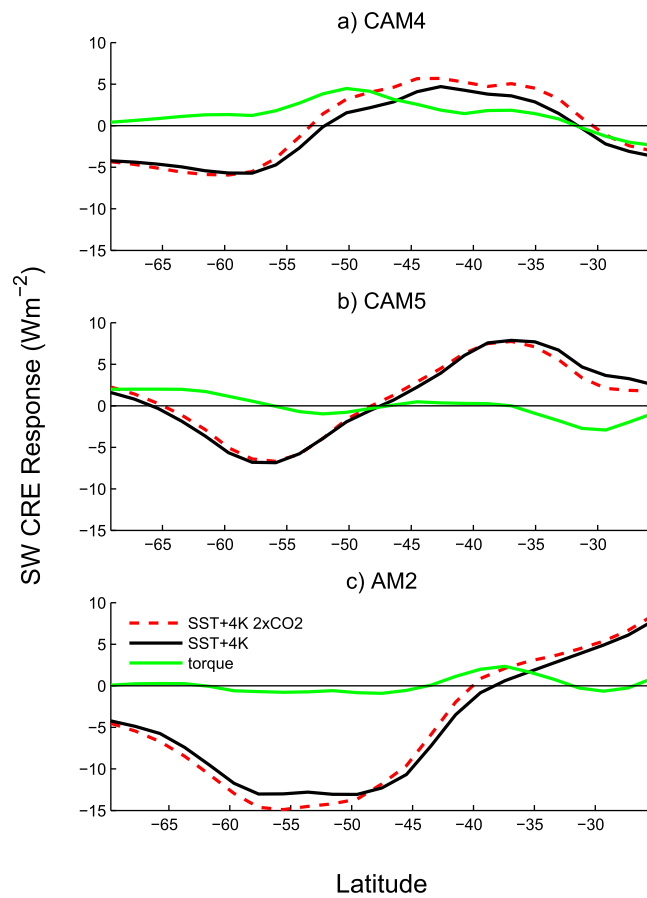


Figure 4. Zonal-mean time-mean SW CRE response to the forcing in the *warming* experiment (with and without a doubling of CO₂) and in the *torque* experiment in (a) CAM4, (b) CAM5, and (c) AM2.

[Rotstayn, 1997; Rotstayn et al., 2000], while CAM5 has a relatively complex “two-moment” scheme that predicts both mixing ratios and droplet/crystal number concentrations of cloud liquid and ice [Morrison and Gettelman, 2008; Gettelman et al., 2010], and includes more processes in the ice microphysics scheme than AM2.

In this study SW CRE is used as an estimate of SW cloud feedback. SW CRE is the difference between the outgoing SW flux for clear sky and all sky conditions. The response of SW CRE to a forcing is related to the shortwave cloud feedback, but not necessarily equal to it because noncloud changes can cause a change in clear sky outgoing SW radiation. Despite this drawback, CRE is generally a good predictor of cloud feedback [Soden et al., 2004; Vial et al., 2013], especially in this study because the surface albedo is held fixed throughout all aquaplanet experiments described above.

3. Results and Discussion

3.1. The Role of Jet Shifts in Extratropical SW Cloud Feedback

The Jet Shift Experiments suggest that the influence of shifts of the eddy-driven jet and the concomitant change in large-scale subsidence/ascent on midlatitude SW cloud feedback varies between models (confirming the results of Kay et al. [2014] and GP14), but in none of the models do jet shifts alone result in a negative response in SW CRE in the high-latitudes that resembles the *warming* response. The response of SW CRE to *torque* and *warming* is shown in Figure 4. First of all, it is important to note that the SW CRE response over the extratropics in the *warming* experiment in all three aquaplanet models is the same order of magnitude and has the same north-south dipole structure as the state of the art CMIP5 models (Figure 1). In two of the models (AM2 and CAM5) the response of SW CRE in the *torque* experiment is small and lacks

In addition to changing the freezing temperature, the saturation vapor pressure seen by the Bergeron process was perturbed. The Bergeron process occurs in mixed-phase clouds when the temperature is slightly below freezing, and results in growth of ice crystals at the expense of liquid droplets. The process occurs because the difference in saturation vapor pressure over liquid and ice is relatively large at temperatures slightly below freezing, which therefore allows states in which the atmosphere is subsaturated with respect to liquid and supersaturated with respect to ice. We therefore perturb the saturation vapor pressure with respect to liquid and ice seen by the Bergeron process only to be consistent with the freezing temperature perturbation applied elsewhere in the code. See Ceppi et al. [2015] for a more thorough description of the method.

The Perturbed Microphysics experiments were run in the AM2 and CAM5 models only. These models were selected because they span the complexity of cloud microphysics parameterizations in current state of the art climate models. AM2 has a relatively simple scheme that predicts mixing ratios of cloud liquid and ice only

the dipole structure when compared to the response in the *warming* experiment, suggesting that changes in large scale circulation alone do not drive significant changes in cloud brightness in the midlatitudes in these models. This is especially clear in the mid- to high-latitudes ($\sim 45^\circ$ – 70°). In CAM4, however, the SW CRE response in the *torque* experiment in the region $\sim 30^\circ$ S– 55° S is of the same order as the SW CRE response in the *warming* experiment. A pronounced positive response in SW CRE (i.e., cloud dimming) occurs between $\sim 30^\circ$ – 55° in the *torque* experiment coinciding with the region where enhanced large-scale subsidence or reduced large-scale ascent occurs (Figure 2). The aquaplanet experiments in this study confirm the results of previous studies in that they suggest that the contribution of large scale circulation changes to SW cloud feedback in the midlatitudes is negligible in some models [Kay *et al.*, 2014], but can be significant in others (GP14). However, the aquaplanet simulations also suggest that circulation changes alone do not produce the cloud brightening at mid- to high-latitudes that is characteristic of warming simulations in GCMs.

Changes in large-scale subsidence do not appear to drive the positive SW cloud feedback in the subtropics and lower midlatitudes in the aquaplanet experiments. Between 30° and 40° S, the ratio of the area integrated SW CRE response in the *torque* experiment to that in the *warming* experiment is -0.16 in CAM5 (i.e., *torque* and *warming* experiments have SW CRE response of opposite sign), 0.28 in CAM4, and 0.35 in AM2, in agreement with previous work suggesting that changes in large-scale subsidence alone are not a dominant mechanism driving subtropical low cloud feedback [Bony *et al.*, 2004; Boucher *et al.*, 2013].

The vertical profile of cloud water changes in these experiments is shown in Figure 5. In all three models, the vertical structure of the cloud response in the *warming* experiment exhibits a vertical dipole pattern that follows the slope of the 273K isotherm. Both the response of cloud liquid and cloud ice mixing ratio exhibit this vertical dipole structure, but the liquid response tends to be larger in magnitude and lower in the atmosphere than the ice response pattern. This spatial structure alone is suggestive of the importance of the phase change mechanism described previously in the text, and will be further discussed in the Perturbed Microphysics experiments below. In the subtropics and lower midlatitudes there is reduced boundary layer cloudiness. This is a common feature of cloud changes with warming in state of the art climate models [Zelinka *et al.*, 2012a].

Figure 5 also shows the vertical structure of the cloud liquid and ice mixing ratio response in the *torque* experiment in the CAM4 model. In the CAM4 model, the poleward jet shift and accompanying large scale subsidence anomalies simulated in the *torque* experiment causes a reduction in low liquid cloud throughout the midlatitudes. The latitudes with reduced low level cloud liquid in the *torque* experiment ($\sim 35^\circ$ S– 55° S) generally coincide with the region of anomalous large scale subsidence ($\sim 35^\circ$ – 50° S) (Figures 2 and 5). The CAM5 and AM2 models show negligible cloud change in the *torque* experiment, and are not shown in Figure 5.

Finally, we note the influence of the direct radiative effect of increasing CO_2 concentrations on SW CRE. An *SST+4K 2xCO₂* experiment was performed in which the SST profile was warmed uniformly by 4K, and CO_2 concentrations were doubled (equivalent to the *warming* experiment with a doubling of CO_2). The difference in SW CRE response between the *warming* and *SST+4K 2xCO₂* experiments shows the change in SW cloud reflection induced by the direct radiative effect of doubling CO_2 . In all three models it is $\sim 1 \text{ Wm}^{-2}$, but, for a given latitude, the sign varies between models. The *warming* and *SST+4K 2xCO₂* experiments both produce a spatial dipole response in SW CRE (Figure 4) and have very similar responses in large-scale extratropical circulation (not shown).

3.2. The Role of Cloud Microphysics in Extratropical SW Cloud Feedback

Having ruled out poleward jet shifts as a mechanism of cloud brightening at mid- to high-latitudes with warming, we now consider the hypothesis that changes in cloud microphysical processes and condensate phase with warming control the negative SW cloud feedback there. As we have already seen, both CMIP5 models (Figure 1) and the aquaplanet models used in this study (Figure 4) predict brighter clouds in the mid- to high-latitudes and dimmer clouds in the subtropics with warming. The positive SW cloud feedback in the subtropics is thought to be controlled by decreasing coverage of low clouds, and to a slightly lesser extent midlevel clouds, which are generally liquid dominated [Zelinka *et al.*, 2012a; Bretherton *et al.*, 2013; Zelinka *et al.*, 2012b]. This behavior appears to be captured in the *warming* experiments in the aquaplanet models as well (Figure 5). If the phase change mechanism does in fact control the cloud brightening response at mid- to high-latitudes in the models, then one might expect that lowering (raising) the freezing

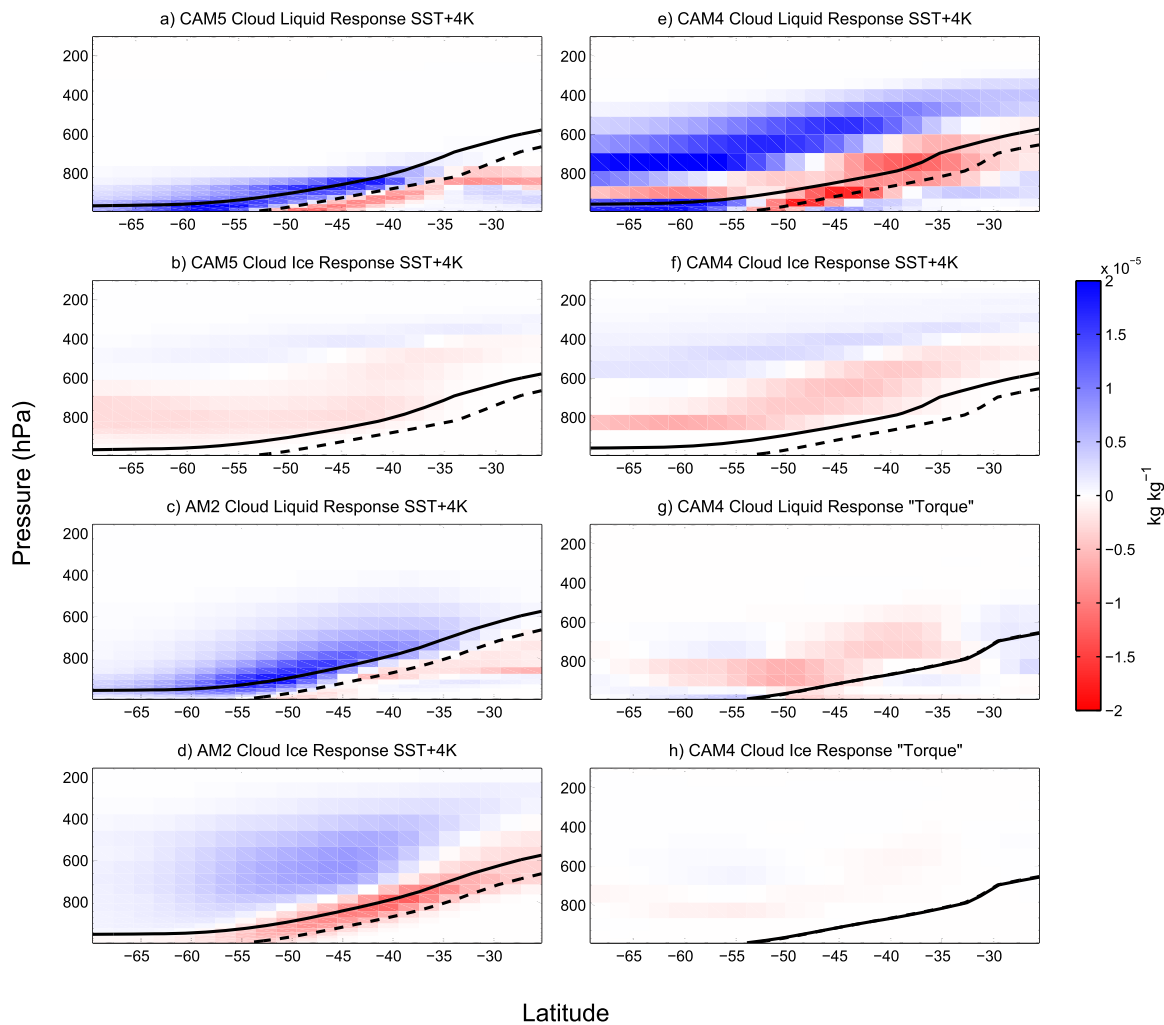


Figure 5. Zonal-mean time-mean response of (a) cloud liquid mixing ratio and (b) ice mixing ratio (color) and freezing isotherm (dashed (thick solid) sloping line indicates the freezing isotherm in the *control* (*warming*) experiment) in CAM5. (c–h) As in Figures 5a and 5b but for the *warming* experiments in AM2 and CAM4 and the *torque* experiment in CAM4, respectively. Cloud changes are negligible in the *torque* experiments in CAM5 and AM2 and are not shown.

temperature seen by the cloud microphysics might cause the negative lobe of the SW cloud feedback dipole pattern to shift to higher (lower) latitudes where the temperatures are colder (warmer), but the positive lobe to exhibit little change. To test this hypothesis we perturb the freezing temperature seen by the ice microphysics in the model from -4°C to $+4^{\circ}\text{C}$ in increments of 1°C and examine the meridional shift of the region of cloud brightening. As a metric for the meridional shift in the negative lobe of the SW cloud feedback dipole pattern, we will use the “dipole crossing latitude,” defined as the latitude at which the cloud response in warming simulations transitions from dimming in the lower midlatitudes to brightening at higher latitudes.

The relationship between the “dipole crossing” latitude, and the freezing temperature perturbation and jet shift is shown in Figure 6. Two models (AM2 and CAM5) and two SST profiles (“QOBS” and “FLAT”) for each model are used in this experiment. AM2 and CAM5 sample the range of complexity in cloud microphysics schemes in current state of the art climate models, with AM2 and CAM5 having relatively simple and complex schemes, respectively. Also, the “QOBS” profile generally produces a climate with a larger bias in the jet latitude than the “FLAT” SST profile. In both models and both SST profiles, the freezing temperature perturbation is highly correlated with the dipole crossing latitude while the jet shift is not significantly correlated with the dipole crossing latitude at the 95% confidence level. The strength of the high-latitude cloud brightening response (computed as the most negative value of the SW CRE response to a uniform SST warming

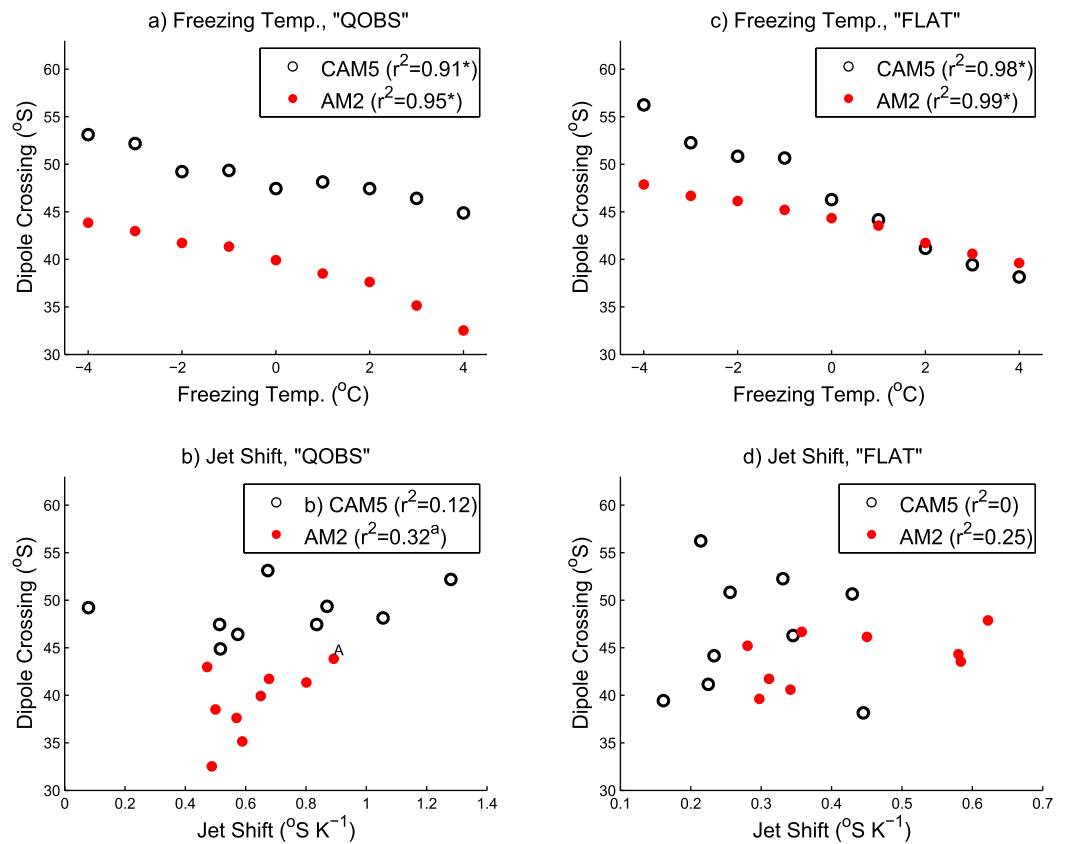


Figure 6. The “dipole crossing” latitude (latitude at which the cloud response in warming simulations transitions from dimming in the lower midlatitudes to brightening in the mid- to high-latitudes) is plotted as a function of (a) freezing temperature perturbation and (b) poleward jet shift from the Perturbed Microphysics Experiments described in the text, using the “QOBS” profile (the same profile used in Jet Shift Experiments). Correlations that are significant at the 95% confidence level are marked with an asterisk. (c, d) As in Figures 6a and 6b but using the “FLAT” SST profile. ^awhen point A is removed from the analysis, $r^2=0.15$. With or without point A the correlation is not significant at the 95% confidence level.

of +4K poleward of 30° S) is also highly correlated with the freezing temperature perturbation (“QOBS” SST profile: $r^2=0.91$ in AM2 and $r^2=0.94$ in CAM5; “FLAT” SST profile: $r^2=0.88$ in AM2, $r^2=0.92$ in CAM5). In both models, lower freezing temperatures are associated with a poleward shift and enhancement of cloud brightening at mid- to high-latitudes in response to warming.

The vertical structure of the cloud liquid mixing ratio response to uniform SST warming of +4K with freezing temperature perturbations of +4°C, 0°C and −4°C, along with the dipole crossing latitude, is shown in Figure 7. As the freezing temperature is perturbed, the regions of mixed-phase clouds shift in space. In both models the cloud liquid mixing ratio response is greatest at temperatures slightly below freezing, and the regions of largest cloud liquid response to warming closely follow the freezing isotherm as it shifts in space.

Taken together, the results of the Jet Shift Experiments and Perturbed Microphysics Experiments suggest that changes in mixed-phase cloud microphysical processes with warming, rather than poleward jet shifts, are the dominant mechanism for SW cloud feedback in the mid- to high-latitudes, confirming the findings of Ceppi *et al.* [2015]. It is also worth noting that the aquaplanet experiments are run without sea ice and still produce a SW cloud feedback north-south dipole in the midlatitudes that is of the same order of magnitude as the fully coupled CMIP5 models. Previous studies have suggested that changes in sea ice cover could cause a negative SW cloud feedback at high-latitudes, as warmer temperatures could cause sea ice cover to shrink, causing more of the ocean surface to be exposed to the atmosphere, which would then result in enhanced moisture flux to the atmosphere and more cloudiness [Fitzpatrick and Warren, 2007; Liu *et al.*, 2012]. These experiments suggest that this mechanism is not necessary in the three models considered in this study.

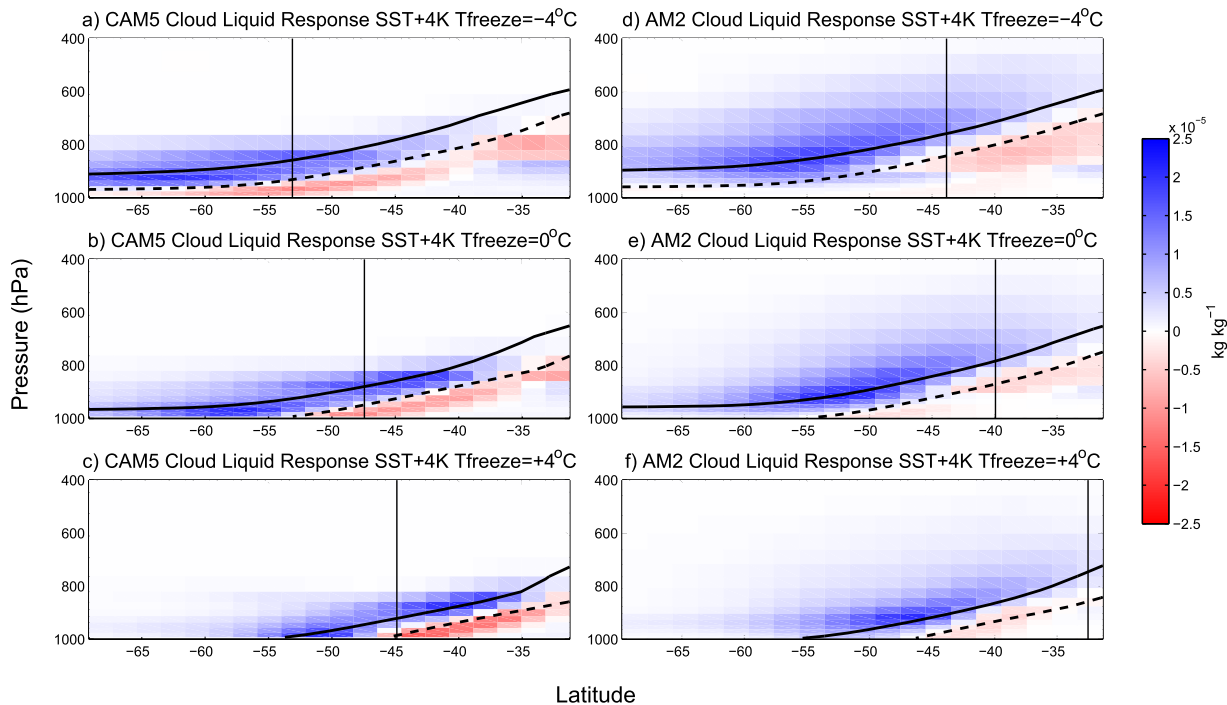


Figure 7. Cloud liquid mixing ratio response (color) to uniform 4K warming of SST with freezing temperatures of (a) -4°C , (b) 0°C and (c) $+4^{\circ}\text{C}$ in CAM5. The dashed (solid) sloped lines show the freezing isotherm seen by the cloud parameterizations in the control (warming) simulation. The vertical line shows the latitude at which the SW CRE response transitions from brightening at higher latitudes to dimming at lower latitudes. (e–g) As in Figures 7a–7c for AM2. The “QOBS” SST profile was used for the experiments shown above.

3.3. Inter-Model Differences in Cloud Response to Jet Shifts Linked to Shallow Convection

We now address the question of why some models exhibit a zonally symmetric cloud dimming pattern throughout the SH midlatitudes associated with a poleward jet shift and some models do not. The CAM4 and CAM5 models are used as a test bed, and we will argue that differences in cloud response to jet shifts in these models arise mainly because of differences in the shallow convection and moist turbulence schemes. In the transition from CAM4 to CAM5, the parameterizations of cloud microphysics, cloud macrophysics, radiation, aerosols, moist turbulence, and shallow convection were updated [Gettelman *et al.*, 2012]. The reason for the different cloud response to a poleward jet shift between CAM4 and CAM5 is not obvious a priori.

In order to diagnose the reason for the difference in cloud response to jet shifts in CAM4 and CAM5 we use a progression of model configurations, which starts from CAM4 and progressively adds one updated moist physics scheme at a time, building up to CAM5 (Table 1). At the time of writing it is not possible to run the CAM4 and CAM5 models with different combinations of moist physics parameterizations from each model. To get around this problem we utilize a set of experiments that were run in the development process of the Community Atmosphere Model in which the parameterizations were updated one at a time from CAM4 to CAM5. Natural variability of the jet latitude and SW CRE in these experiments is analyzed. All runs were performed with an atmosphere-only model with SSTs fixed to a monthly climatology based on observations, CO_2 concentrations fixed at 280 ppmv, and run for 5–10 years. We emphasize that these experiments were run with SSTs prescribed to a monthly climatology, while the aquaplanet experiments described earlier in this study were run with zonally symmetric SST profiles that did not vary in time.

In order to test the sensitivity of SW CRE to variations in the jet latitude, SW CRE was regressed on jet latitude for the different model configurations making up the progression from CAM4 to CAM5. This was done by computing the latitude of the jet maximum, ϕ , computing the zonal mean SW CRE, and removing the mean and seasonal cycle from each to get ϕ' and SW CRE' respectively (see Appendix A). Data from December, January, and February (DJF) were then used to compute the regression of SW CRE' on ϕ' . At each latitude the 95% confidence interval for the regression coefficient was computed using an estimate of the effective sample size, which was computed following the method of Bretherton *et al.* [1999]. It is important

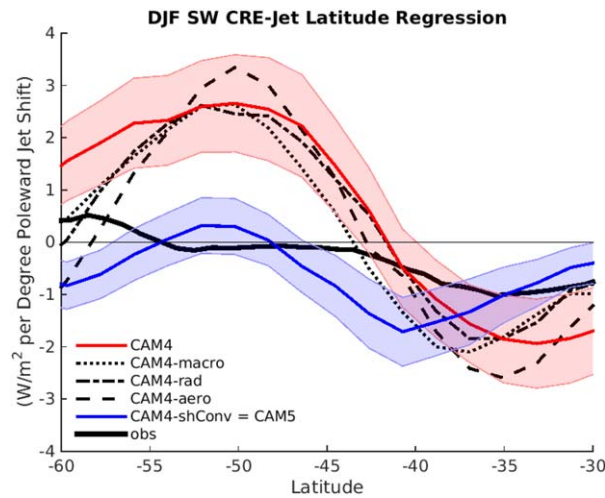


Figure 8. Regression coefficient of December January February (DJF) anomalies of SH jet latitude and zonal mean SW CRE for a progression of model configurations building up from CAM4 to CAM5 and observations from 2000 to 2014 of SW CRE from CERES and zonal wind from ERA-Interim reanalysis. Models are ordered in the legend such that one update at a time is added progressively from top to bottom, building up from CAM4 to CAM5 (Table 1). The sign convention is such that a positive regression coefficient indicates that a poleward jet shift is associated with a positive anomaly in SW CRE (i.e., a dimming of the clouds). Additionally, 95% confidence intervals for the regression coefficients are shown for CAM4 and CAM5-shConv (equivalent to CAM5).

(upward) motion at 500 hPa associated with a poleward jet shift (not shown). This is consistent with the findings of the Jet Shift Experiments, where the CAM4 aquaplanet model showed significant cloud dimming in regions of anomalous large scale subsidence as the circulation shifted poleward. In CAM5, on the other hand, regression coefficients of SW CRE' on ϕ' between 45°S and 60°S are either not significantly different from zero or are small and negative, confirming the findings of Kay *et al.* [2014]. The regression coefficients of DJF zonal mean SW CRE on jet latitude in CAM4 and CAM5 are significantly different at the 95% confidence level between 45°S and 60°S (Figure 8). All of the model configurations in the progression up to CAM4-aero (CAM4 with all updates except for shallow convection and moist turbulence) show regression patterns that closely resemble CAM4, indicating that the updated shallow convection and moist turbulence schemes in CAM5 are responsible for the different sensitivities of SW CRE to jet shifts in the models.

It is perhaps not surprising that differences in shallow convective mixing can impact the response of SW CRE to a shift in the eddy-driven jet. It has been shown that the strength of convective mixing between the boundary layer and free troposphere has a strong influence on the magnitude of SW cloud feedback in the tropics, and likely the midlatitudes as well [Sherwood *et al.*, 2014]. Therefore, one might expect the differences in shallow convection and moist turbulence schemes, which contribute to the strength of mixing between the boundary layer and free troposphere in the extratropics, may have an important role in the component of SW cloud feedback induced by a poleward jet shift. Also, note that in the Jet Shift Experiments, the cloud response in the *torque* experiment in CAM4 is dominated by a decrease in cloud liquid water content in the lower troposphere, where the shallow convection scheme is most active (Figure 5).

Observations from March 2000 to February 2014 of DJF monthly mean SW CRE from CERES and jet latitude from ERA-Interim reanalysis are shown in Figure 8. The regression coefficients between DJF zonal mean SW CRE and jet latitude anomalies at latitudes between 45°S and 60°S from observations are not significantly different from zero at the 95% confidence level. The spatial pattern of the regression coefficients of CAM5 is in closer agreement with observations than CAM4. This result is consistent with GP14, who compared models in which a poleward jet shift is associated with a strong zonally symmetric cloud dimming in the midlatitudes ("CAM4-like models") and models in which it is not ("CAM5-like models") and found that "CAM5-like models" generally show better agreement with observations than "CAM4-like models."

to note that the DJF jet latitude mean and standard deviation are not significantly different between model configurations (Table 1).

The regression coefficients of SW CRE' on ϕ' for the different models in the CAM4 to CAM5 progression are shown in Figure 8 and reveal that the updated moist turbulence and shallow convection schemes are the reason for the different responses of SW CRE to jet shifts in CAM4 and CAM5 [see Park and Bretherton, 2009; Bretherton and Park, 2009] for descriptions of the updated shallow convection and moist turbulence schemes, respectively). CAM4 has a spatial dipole pattern in the regression coefficients, with positive coefficients of $\sim 2 \text{ Wm}^{-2}$ per degree poleward jet shift in the mid- to high-latitudes ($\sim 45^\circ\text{S}$ – 60°S) and negative regression coefficients in the lower midlatitudes ($\sim 45^\circ\text{S}$ – 30°S), consistent with the findings of GP14. Between $\sim 45^\circ\text{S}$ – 60°S ($\sim 45^\circ\text{S}$ – 30°S), where a poleward jet shift is associated with cloud dimming (brightening), there is also anomalous downward

4. Conclusion

Warming simulations in GCMs, including the aquaplanet models used in this study and fully coupled CMIP5 models, show a robust SW cloud feedback dipole in the Southern Hemisphere extratropics, with a negative feedback in the high-latitudes and a positive feedback in the subtropics. The results of this study suggest that the negative SW cloud feedback at high-latitudes is driven by changes in cloud ice microphysical processes, rather than jet shifts, confirming the findings of previous studies [Kay et al., 2014; Ceppi et al., 2015; GP14]. In the subtropics, however, the role of poleward jet shift/Hadley cell expansion in driving the positive SW cloud feedback varies greatly between models, and in the two models tested in this study, the difference results largely from inter-model differences in the shallow convection parameterization.

Further evaluation of cloud microphysics in GCMs may significantly reduce uncertainty in high-latitude SW cloud feedback. Cloud microphysics are represented by parameterizations that differ largely between GCMs [Tsushima et al., 2006]. For example, McCoy et al. [2015] found that the average temperature at which CMIP5 models produce clouds with equally mixed liquid and ice (the “glaciation temperature”) over the Southern Ocean varies by over 40K between models. In this study it is demonstrated that the glaciation temperature (which is perturbed by way of perturbing the freezing temperature) in both AM2 and CAM5 is highly correlated with the latitude and strength of the negative SW cloud feedback at mid- to high-latitudes, such that lower glaciation temperature corresponds to a poleward shift and strengthening of the negative SW feedback at mid- to high-latitudes. We therefore hypothesize that narrowing both the bias and inter-model spread in glaciation temperature will constrain the strength and latitude of the negative SW cloud feedback at high-latitudes in GCMs.

Additionally, further evaluation of inter-model differences in shallow convection schemes is likely to reduce inter-model spread in SW cloud feedback in the midlatitudes. It has previously been demonstrated that convective mixing between the boundary layer and the free troposphere in the tropics can explain a large amount of variance in climate sensitivity and cloud feedback between GCMs [Sherwood et al., 2014]. Here we further demonstrate that shallow convection can play a role in inter-model differences in SW cloud feedback in the extratropics.

Appendix A

A1. Zonal Wind Tendency in Jet Shift Experiments

In this section, a detailed description of the zonal wind tendency in the *torque* experiment is given. In summary, the model was forced with a zonally uniform, steady zonal wind tendency perturbation τ that was located in both hemispheres in the midlatitude upper troposphere, poleward of the eddy-driven jet maximum in the *control* experiment. The zonal wind tendency was prescribed as:

$$\tau(\phi, p) = Ah(p) \exp\left(-\frac{(|\phi| - \phi_0)^2}{2L^2}\right)$$

where A is the amplitude of the perturbation, $h(p)$ is the pressure dependence (defined below), ϕ is latitude, ϕ_0 the latitude of the perturbation center, and L is the meridional length scale of the perturbation. The pressure dependence of the perturbation was prescribed as:

$$h(p) = \begin{cases} \cos\left(\frac{\pi(p-p_0)}{H}\right), & |p-p_0| \leq H/2 \\ 0, & \text{else} \end{cases}$$

where p is the atmospheric pressure, p_0 is the pressure of the torque center, and H is the vertical length scale of the perturbation. Finally, one line of code was added to the end of the dynamical core of the model in order to apply the zonal wind perturbation at each time step:

$$u(\phi, \lambda, p, t) = u(\phi, \lambda, p, t) + \tau(\phi, p)dt$$

Table A1. Parameters Used in the Jet Shift Experiments

Model	A ($\text{ms}^{-1}\text{day}^{-1}$)	ϕ_0 ($^{\circ}\text{N/S}$)	L ($^{\circ}\text{N/S}$)	p_0 (hPa)	H (hPa)
CAM5	1.4	50	4	250	400
CAM4	0.8	52	4	250	400
AM2	1.2	47	4	250	400

where λ is longitude. The values of the parameters used in each model are listed in Table A1.

A2. Method to Compute SW CRE-Jet Latitude Regression

In order to compute the SW CRE-jet latitude regression coefficients the method of GP14 was followed with two exceptions: zonal mean SW CRE was considered instead of computing regression coefficients at every grid point and the seasonal cycle was removed by removing the first three harmonics corresponding to the annual cycle in the Fourier transform of the signal instead of a compositing method used in GP14. The Fourier method used in this study is better suited for the model output analyzed in this study because model runs are only 5–10 years long.

The jet latitude was computed using the method of GP14: (1) the gridpoint i of the zonal mean, zonal wind maximum was located; (2) a quadratic fit was performed using the zonal mean, zonal wind maximum and the two neighboring gridpoints: $i-1$, i and $i+1$; (3) the jet latitude, ϕ , was defined as the maximum of the quadratic fit.

The SW CRE-jet latitude regression coefficients were computed as follows: (1) the mean and seasonal cycle of the ϕ timeseries and the SW CRE timeseries at each gridpoint i, j were removed resulting in the deseasonalized timeseries ϕ' and $SW\ CRE'_{i,j}$ respectively. The seasonal cycle was removed by removing the first three harmonics corresponding to the annual cycle in the Fourier transform of the corresponding timeseries; (2) $\overline{SW\ CRE}'_i$, the zonal mean of $SW\ CRE'_{i,j}$ was computed; (3) values from December, January and February were used to compute regression coefficients of $\overline{SW\ CRE}'_i$ on ϕ' at each latitude point.

Acknowledgments

We thank Paulo Ceppi for helpful discussion and providing code to perturb freezing temperature in the models, Andrew Gettelman for providing data from the "Modified Cess" experiments and valuable insight, Daniel McCoy and Chris Bretherton for helpful discussion, Mark Zelinka for providing CMIP5 SW cloud feedback data, Marc Michelsen for computer support and reviewers for their feedback. This study was supported by the National Science Foundation (grant AGS-0960497). The source code for the models used in this study, CAM4/CAM5 and AM2, is freely available at http://www.cesm.ucar.edu/models/cesm1.0/cesm/cesm_doc_1_0_4/x350.html and <http://www.gfdl.noaa.gov/am3>, respectively. Both the data and input files necessary to reproduce the experiments are available from the authors upon request (caseyw8@atmos.washington.edu). All other data used in this study are properly cited in Table 1.

References

- Anderson, J. L., et al. (2004), The new GFDL global atmosphere and land model AM2-LM2: Evaluation with prescribed SST simulations, *J. Clim.*, *17*, 4641–4673, doi:10.1175/JCLI-3223.1.
- Barnes, E. A., and L. Polvani (2013), Response of the midlatitude jets, and of their variability, to increased greenhouse Gases in the CMIP5 Models, *J. Clim.*, *26*(18), 7117–7135, doi:10.1175/JCLI-D-12-00536.1.
- Bender, F. A. M., V. Ramanathan, and G. Tselioudis (2012), Changes in extratropical storm track cloudiness 1983–2008: Observational support for a poleward shift, *Clim. Dyn.*, *38*(9–10), 2037–2053, doi:10.1007/s00382-011-1065-6.
- Betts, A. K., and Harshvardhan (1987), Thermodynamic constraint on the cloud liquid water feedback in climate models, *J. Geophys. Res.*, *92*, 8483–8485.
- Blackburn, M., and B. J. Hoskins (2013), Context and aims of the aqua-planet experiment, *J. Meteorol. Soc. Jpn.*, *91A*, 1–15, doi:10.2151/jmsj.2013-A01.
- Bony, S., and J.-L. Dufresne (2005), Marine boundary layer clouds at the heart of tropical cloud feedback uncertainties in climate models, *Geophys. Res. Lett.*, *32*, L20806, doi:10.1029/2005GL023851.
- Bony, S., J.-L. Dufresne, H. Le Treut, J.-J. Morcrette, and C. Senior (2004), On dynamic and thermodynamic components of cloud changes, *Clim. Dyn.*, *22*(2–3), 71–86, doi:10.1007/s00382-003-0369-6.
- Bony, S., et al. (2015), Clouds, circulation and climate sensitivity, *Nat. Geosci.*, *8*(4), 261–268, doi:10.1038/ngeo2398.
- Boucher, O., et al. (2013), Clouds and aerosols, in *Climate Change 2013: The Physical Science Basis, Contribution of Working Group I to the Fifth Assessment Report of the Intergovernmental Panel on Climate Change*, edited by T. F. Stocker et al., pp. 578–595, Cambridge Univ. Press, Cambridge, U. K.
- Bretherton, C. S., and S. Park (2009), A new moist turbulence parameterization in the community atmosphere model, *J. Clim.*, *22*, 3422–3448, doi:10.1175/2008JCLI2556.1.
- Bretherton, C. S., M. Widmann, V. P. Dymnikov, J. M. Wallace, and I. Blade (1999), Effective number of degrees of freedom of a spatial field, *J. Clim.*, *12*(1969), 1990–2009, doi:10.1175/1520-0442(1999)012<1990:Tenosd>2.0.Co;2.
- Bretherton, C. S., P. N. Blossey, and C. R. Jones (2013), Mechanisms of marine low cloud sensitivity to idealized climate perturbations: A single-LES exploration extending the CGILS cases, *J. Adv. Model. Earth Syst.*, *5*, 316–337, doi:10.1002/jame.20019.
- Brient, F., and S. Bony (2012), Interpretation of the positive low-cloud feedback predicted by a climate model under global warming, *Clim. Dyn.*, *40*(9–10), 2415–2431, doi:10.1007/s00382-011-1279-7.
- Ceppi, P., and D. L. Hartmann (2015), Connections between clouds, radiation, and midlatitude dynamics: A review, *Curr. Clim. Change Rep.*, *1*(2), 94–102, doi:10.1007/s40641-015-0010-x.
- Ceppi, P., Y.-T. Hwang, D. M. W. Frierson, and D. L. Hartmann (2012), Southern Hemisphere jet latitude biases in CMIP5 models linked to shortwave cloud forcing, *Geophys. Res. Lett.*, *39*, L19708, doi:10.1029/2012GL053115.
- Ceppi, P., M. D. Zelinka, and D. L. Hartmann (2014), The response of the Southern Hemisphere eddy-driven jet to future changes in shortwave radiation in CMIP5, *Geophys. Res. Lett.*, *41*, 3244–3250, doi:10.1002/2014GL060043.
- Ceppi, P., D. Hartmann, and M. Webb (2015), Mechanisms of the negative shortwave cloud feedback in high latitudes, *J. Clim.*, doi:10.1175/JCLI-D-15-0327.1, in press.
- Cess, R., et al. (1990), Intercomparison and interpretation of cloud-climate feedback processes in nineteen atmospheric general circulation models, *J. Geophys. Res.*, *95*, 16,601–16,615.
- Colman, R. (2003), A comparison of climate feedbacks in general circulation models, *Clim. Dyn.*, *20*, 865–873.
- Dee, D. P., et al. (2011), The ERA-Interim reanalysis: Configuration and performance of the data assimilation system, *Q. J. R. Meteorol. Soc.*, *137*, 553–597, doi:10.1002/qj.828.
- Fitzpatrick, M. F., and S. G. Warren (2007), The relative importance of clouds and sea ice for the solar energy budget of the Southern Ocean, *J. Clim.*, *20*(6), 941–954, doi:10.1175/JCLI4040.1.
- Gettelman, A., X. Liu, S. J. Ghan, H. Morrison, S. Park, A. J. Conley, S. A. Klein, J. Boyle, D. L. Mitchell, and J.-L. F. Li (2010), Global simulations of ice nucleation and ice supersaturation with an improved cloud scheme in the Community Atmosphere Model, *J. Geophys. Res.*, *115*, D18216, doi:10.1029/2009JD013797.

- Gettelman, A., J. E. Kay, and K. M. Shell (2012), The evolution of climate sensitivity and climate feedbacks in the community atmosphere model, *J. Clim.*, *25*(5), 1453–1469, doi:10.1175/JCLI-D-11-00197.1.
- Gordon, N. D., and S. A. Klein (2014), Low-cloud optical depth feedback in climate models, *J. Geophys. Res. Atmos.*, *119*, 6052–6065, doi:10.1002/2013JD021052.
- Grise, K. M., and L. M. Polvani (2014), Southern Hemisphere cloud–dynamics biases in CMIP5 models and their implications for climate projections, *J. Clim.*, *27*(15), 6074–6092, doi:10.1175/JCLI-D-14-00113.1.
- Grise, K. M., L. M. Polvani, G. Tselioudis, Y. Wu, and M. D. Zelinka (2013), The ozone hole indirect effect: Cloud-radiative anomalies accompanying the poleward shift of the eddy-driven jet in the Southern Hemisphere, *Geophys. Res. Lett.*, *40*, 3688–3692, doi:10.1002/grl.50675.
- Haynes, J. M., C. Jakob, W. B. Rossow, G. Tselioudis, and J. Brown (2011), Major characteristics of southern ocean cloud regimes and their effects on the energy budget, *J. Clim.*, *24*(19), 5061–5080, doi:10.1175/2011JCLI4052.1.
- Held, I. M., and B. J. Soden (2006), Robust responses of the hydrological cycle to global warming, *J. Clim.*, *19*(21), 5686–5699, doi:10.1175/JCLI3990.1.
- Hwang, Y.-T., and D. M. W. Frierson (2013), Link between the double-Intertropical Convergence Zone problem and cloud biases over the Southern Ocean, *Proc. Natl. Acad. Sci. U. S. A.*, *110*(13), 4935–4940, doi:10.1073/pnas.1213302110.
- Kay, J. E., B. Medeiros, Y. T. Hwang, A. Gettelman, J. Perket, and M. G. Flanner (2014), Processes controlling Southern Ocean shortwave climate feedbacks in CESM, *Geophys. Res. Lett.*, *5*, 616–622, doi:10.1002/2013GL058315.
- Li, Y., D. W. J. Thompson, G. L. Stephens, and S. Bony (2014), A global survey of the instantaneous linkages between cloud vertical structure and large-scale climate, *J. Geophys. Res. Atmos.*, *119*, 3770–3792, doi:10.1002/2013JD020669.
- Liu, Y., J. R. Key, Z. Liu, and X. Wang, and S. J. Vavrus (2012), A cloudier Arctic expected with diminishing sea ice, *Geophys. Res. Lett.*, *39*, L05705, doi:10.1029/2012GL051251.
- Loeb, N. G., S. Kato, W. Su, T. Wong, F. G. Rose, D. R. Doelling, J. R. Norris, and X. Huang (2012), Advances in understanding top-of-atmosphere radiation variability from satellite observations, *Surv. Geophys.*, *33*, 359–385, doi:10.1007/s10712-012-9175-1.
- McCoy, D. T., D. L. Hartmann, and D. P. Grosvenor (2014), Observed Southern Ocean cloud properties and shortwave reflection Part 2: Phase changes and low cloud feedback, *J. Clim.*, *27*, 8858–8868, doi:10.1175/JCLI-D-14-00288.1.
- McCoy, D. T., D. L. Hartmann, M. D. Zelinka, P. Ceppi, and D. P. Grosvenor (2015), Mixed-phase cloud physics and Southern Ocean cloud feedback in climate models, *J. Geophys. Res. Atmos.*, *120*, 9539–9554, doi:10.1002/2015JD023603.
- Medeiros, B., B. Stevens, I. M. Held, M. Zhao, D. L. Williamson, J. G. Olson, and C. S. Bretherton (2008), Aquaplanets, climate sensitivity, and low clouds, *J. Clim.*, *21*, 4974–4991, doi:10.1175/2008JCLI1995.1.
- Medeiros, B., B. Stevens, and S. Bony (2014), Using aquaplanets to understand the robust responses of comprehensive climate models to forcing, *Clim. Dyn.*, 1957–1977, doi:10.1007/s00382-014-2138-0.
- Morrison, H., and A. Gettelman (2008), A new two-moment bulk stratiform cloud microphysics scheme in the Community Atmosphere Model, Version 3 (CAM3). Part I: Description and numerical tests, *J. Clim.*, *21*(15), 3642–3659, doi:10.1175/2008JCLI2105.1.
- Morrison, H., G. de Boer, G. Feingold, J. Harrington, M. D. Shupe, and K. Sulia (2011), Resilience of persistent Arctic mixed-phase clouds, *Nat. Geosci.*, *5*(1), 11–17, doi:10.1038/ngeo1332.
- Neale, R. B., and B. J. Hoskins (2000), A standard test for AGCMs including their physical parametrizations: I: The proposal, *Atmos. Sci. Lett.*, *1*(2), 101–107, doi:10.1006/asle.2000.0019.
- Neale, R. B., et al. (2010a), Description of the NCAR Community Atmosphere Model (CAM 5.0), *NCAR Tech. Note NCAR/TN-486-STR*, 268 pp. [Available at http://www.cesm.ucar.edu/models/cesm1.0/cam/docs/description/cam5_desc.pdf].
- Neale, R. B., et al. (2010b), Description of the NCAR Community Atmosphere Model (CAM 4.0), *NCAR Tech. Note NCAR/TN-485-STR*, 212 pp. [Available at http://www.cesm.ucar.edu/models/ccsm4.0/cam/docs/description/cam4_desc.pdf].
- Park, S., and C. S. Bretherton (2009), The University of Washington shallow convection and moist turbulence schemes and their impact on climate simulations with the community atmosphere model, *J. Clim.*, *22*(12), 3449–3469, doi:10.1175/2008JCLI2557.1.
- Rotstayn, L. D. (1997), A physically based scheme for the treatment of stratiform clouds and precipitation in large-scale models. I: Description and evaluation of the microphysical processes, *Q. J. R. Meteorol. Soc.*, *123* (541), 1227–1282, doi:10.1002/qj.49712354106.
- Rotstayn, L. D., B. F. Ryan, and J. J. Katzfey (2000), A scheme for calculation of the liquid fraction in mixed-phase stratiform clouds in large-scale models, *Mon. Weather Rev.*, *128*(4), 1070–1088, doi:10.1175/1520-0493(2000)128<1070:ASFcot>2.0.CO;2.
- Senior, C. A., and J. F. B. Mitchell (1993), Carbon dioxide and climate: The impact of cloud parameterization, *J. Clim.*, *6*, 393–418.
- Sherwood, S. C., S. Bony, and J.-L. Dufresne (2014), Spread in model climate sensitivity traced to atmospheric convective mixing, *Nature*, *505*(7481), 37–42, doi:10.1038/nature12829.
- Soden, B. J., A. J. Broccoli, and R. S. Hemler (2004), On the use of cloud forcing to estimate cloud feedback, *J. Clim.*, *17*, 3661–3665, doi:10.1175/1520-0442(2004)017<3661:OTUOCF>2.0.CO;2.
- Soden, B. J., I. M. Held, R. Colman, K. M. Shell, J. T. Kiehl, and C. A. Shields (2008), Quantifying climate feedbacks using radiative kernels, *J. Clim.*, *21*(14), 3504–3520, doi:10.1175/2007JCLI2110.1.
- Tao, L., Y. Hu, and J. Liu (2015), Anthropogenic forcing on the Hadley circulation in CMIP5 simulations, *Clim. Dyn.*, doi:10.1007/s00382-015-2772-1.
- Taylor, K. E., R. J. Stouffer, and G. A. Meehl (2012), An overview of CMIP5 and the experiment design, *Bull. Am. Meteorol. Soc.*, *93*(4), 485–498, doi:10.1175/BAMS-D-11-00094.1.
- Tselioudis, G., and W. B. Rossow (2006), Climate feedback implied by observed radiation and precipitation changes with midlatitude storm strength and frequency, *Geophys. Res. Lett.*, *33*, L02704, doi:10.1029/2005GL024513.
- Tsushima, Y. et al. (2006), Importance of the mixed-phase cloud distribution in the control climate for assessing the response of clouds to carbon dioxide increase: A multi-model study, *Clim. Dyn.*, *27*(2–3), 113–126, doi:10.1007/s00382-006-0127-7.
- Vial, J., Dufresne, J. L., and S. Bony (2013), On the interpretation of inter-model spread in CMIP5 climate sensitivity estimates, *Clim. Dyn.*, *41*, 3339–3362, doi:10.1007/s00382-013-1725-9.
- Voigt, A., and T. A. Shaw (2015), Circulation response to warming shaped by radiative changes of clouds and water vapour, *Nat. Geosci.*, *8*, 102–106, doi:10.1038/ngeo2345.
- Zelinka, M. D., S. A. Klein, and D. L. Hartmann (2012a), Computing and partitioning cloud feedbacks using cloud property histograms. Part I: Cloud Radiative Kernels, *J. Clim.*, *25*(11), 3715–3735, doi:10.1175/JCLI-D-11-00248.1.
- Zelinka, M. D., S. A. Klein, and D. L. Hartmann (2012b), Computing and partitioning cloud feedbacks using cloud property histograms. Part II: Attribution to changes in cloud amount, altitude, and optical depth, *J. Clim.*, *25*(11), 3736–3754, doi:10.1175/JCLI-D-11-00249.1.